



Synthesis and characterization of nanosized CuO-SnO₂ and CuO-SnO₂-Fe₂O₃ Mixed Metal Oxides

M. J. Devade

Department of Chemistry, Jijamata Mahavidyalaya, Buldana-443001, M.S., **INDIA**

Email: mareshdevade@hotmail.com

Accepted on 19th January 2015

ABSTRACT

Mixed metal oxides (MMOs) have been widely used for various applications such as catalysts in organic synthesis, new materials that can be used as electrodes in electrochemical double layer capacitors (EDLC) or super capacitors. This work presents synthesis of a group of mixed metal oxides (CuO-SnO₂ and CuO-SnO₂-Fe₂O₃) by employing simple synthesis technique namely; hydrothermal method. The prepared MMOs were characterized using X-ray diffraction, infra-red spectroscopy, TG-DTA and scanning electron microscopy. The obtained XRD results showed that single phase double oxide compounds were the main components in each case and extent of crystallization of the both MMOs. From SEM images it is clear that CuO-SnO₂ and CuO-SnO₂-Fe₂O₃ particles were obtained in nano size range and showed uniform-sized particles with somewhat spherical morphology.

Keywords: Mixed metal oxides, Catalysis, Nanochemistry, Transition and noble group metals.

INTRODUCTION

Metal oxides represent one of the most important and widely employed categories of solid catalysts, either as active phases or as supports. Metal oxides are utilized both for their acid-base and redox properties and constitute the largest family of catalysts in heterogeneous catalysis [1]. Metals and metal oxides form the bulk of catalysts employed for many synthetic conversions. Transition and noble group metals are frequently used as catalysts and their activity has been attributed to the outer electron configuration [2]. Single metal oxides can crystallize with different morphologies (isotropic, anisotropic or amorphous) and local co-ordination. All metal oxides can crystallize at room temperature, but many phases may remain amorphous at modest calcinations temperatures. The majority of one component metal oxides crystallize with an isotropic morphology (without preferential orientation) and the surface may terminate with M-OH, M-O-M, MQO or M-() functionalities where M-() represents an oxygen vacancy. Among the metal oxide catalysts, those of transition metals occupy a predominant place owing to their low cost of production, easy regeneration and selective action. They are used in widely different types of organic reactions, such as oxidation, dehydration, dehydrogenation and isomerization. Their catalytic activity may be traced to the presence of partially filled d-shells of the metal ion and to the influence of the oxide ligand field on this partially filled d-shell. In the view of a catalytic chemist, mixed metal oxides are oxygen-containing combinations of two or more metallic ions in proportions that may either vary or be defined by

a strict stoichiometry. Solid solutions and mixed metal oxides are classified by physicochemists according to their crystalline systems. Mixed metal oxides are generally obtained in the form of powder or single crystals. They have a wide spectrum of industrial applications in ceramics, electronics, nuclear research and especially in catalysis [3]. Since last one decade, there has been focus on synthesis and applications of mixed metal oxides. They were used for selective reduction of CQO in α,β -unsaturated carbonyls through catalytic hydrogen transfer reaction[4], study of chemical structures and performance of perovskite oxides [5], epoxidation on $\text{MoO}_3/\text{TiO}_2$ oxide [6a], study of effect of phosphate ions on the textural and catalytic activity of titania–silica mixed oxide [6b]. Recently Jackson and Hargreaves published a book on mixed metal oxides [7a]. Due to the versatility in chemical and physical properties along with wide applications in the field of synthesis and technology, the mixed metal oxides (MMOs) secure their own position in heterogenous catalysis [8-12]. The most important and widely employed classes of solid catalysts, either as active phases or support are represented by mixed metal oxides. In heterogenous catalysis, mixed metal oxides are applied for both their acid-base and redox properties and thus represents the largest family of catalysts [13-15]. The deposition of one oxide over another oxide is the interesting phenomenon. Various methods such as sol-gel [16-18], wet impregnation [19,20], mechanochemical synthesis [21], hydrothermal method [22,23], co-precipitation [24,25] etc. are well known for the preparation of MMOs. Nano sized iron- cerium mixed oxides with diameters ranging from 10-20 nm by slow addition of precipitating agent and its application in photocatalyst for dye degradation have been reported by Parida et.al [26]. An et al. reported the nanometer coupled oxide ZnO-SnO_2 using the co-precipitation method, with slow addition of aqueous ammonia [27]. The nanosized ZnO-SnO_2 with high photo catalysis activity by using slow addition of NaOH as precipitating agent with vigorous stirring documented by Zhang and co-workers [28], Yoo and co-workers synthesized MgO-CeO_2 mixed oxide catalyst by using ionic liquid and NaOH as co-precipitating agent for dimethyl carbonate synthesis [29]. Israel E. Wachs and Kamalakanta Routray reviewed the traditional concepts that have been employed to explain catalysis by bulk mixed oxides (molybdates, vanadates, spinels, perovskites, and several other specific mixed oxide systems) and introduces a modern perspective to the fundamental surface structure–activity/selectivity relationships for bulk mixed oxide catalysts[30].

Very recently Kadir et.al have explained the use of SnO_2 through presentation of H_2 gas sensors based on hollow and filled, well aligned electrospun SnO_2 nanofibers, operating at a low temperature of 150 °C [31] In continuation of the efforts for of the facts about behavior and properties of oxides, in this paper we have report hydrothermal synthesis of CuO-SnO_2 and $\text{CuO-SnO}_2\text{-Fe}_2\text{O}_3$ mixed metal oxides using urea as the hydrolytic agent. The prepared CuO-SnO_2 and $\text{CuO-SnO}_2\text{-Fe}_2\text{O}_3$ catalysts were characterized by several analytical techniques such as XRD, FTIR, TG-DTA and SEM.

MATERIALS AND METHODS

Synthesis of CuO-SnO_2 mixed oxide: $\text{Cu}(\text{NO}_3)_2 \cdot 3\text{H}_2\text{O}$ (0.05 mol) and $\text{SnCl}_2 \cdot 2\text{H}_2\text{O}$ (0.05 mol) were initially dissolved in 250 mL of water and then urea (0.2 mol) was added to the homogeneous mixture and transferred to an autoclave. The solution was allowed to reach to 180 °C within an hour (ramp time). The reaction was kept at this temperature for 2 h (soak time) with an in-situ pressure of 12 atmospheres. After 2 h, it was cooled to room temperature. The product was filtered, washed with water and acetone and dried at 110°C in a hot air oven. The initial pH of the experimental solution was acidic (pH ~ 4) and the final pH was alkaline (pH ~8). The final product was pale green in color.

Synthesis of $\text{CuO-SnO}_2\text{-Fe}_2\text{O}_3$ mixed oxide: $\text{Cu}(\text{NO}_3)_2 \cdot 3\text{H}_2\text{O}$ (0.05 mol), $\text{FeCl}_2 \cdot 4\text{H}_2\text{O}$ (0.05 mol) and $\text{SnCl}_2 \cdot 2\text{H}_2\text{O}$ (0.05 mol) were initially dissolved in 250 mL of water and then urea (0.2 mol) was added to the homogeneous mixture and transferred to an autoclave. The solution was allowed to reach to 180 °C within an hour (ramp time). The reaction was kept at this temperature for 2 h (soak time) with an in-situ pressure of 12 atmospheres. After 2 h, it was cooled to room temperature. The product was filtered, washed with water and acetone and dried at 110 °C in a hot air oven. The initial pH of the experimental

solution was acidic (pH ~ 4) and the final pH was alkaline (pH ~8). The final powder was reddish brown in color.

Characterization of CuO-SnO₂ and CuO-SnO₂-Fe₂O₃: After calcinations, the catalyst was characterized by various analytical and spectroscopic techniques. The X-ray powder diffraction pattern was obtained using the conventional powder diffractometer (Rigaku Miniflex II) using graphite monochromatized Cu-K α radiation operating in Bragg-Brentano ($\theta/2\theta$) geometry. Thermogravimetric analysis (TGA) and Differential thermal analysis (DTA) under nitrogen atmosphere were carried out by using Perkin Elmer, USA Model- Diamond TG/DTA. The thermal traces under air (static) atmosphere were recorded employing mettler Toledo star instruments. The Fourier transform infrared spectrum (FT-IR) of the sample was recorded on a Bruker, Germany 3000 Hyperion Microscope with Vertex 80 FTIR System using KBr pellet. Scanning Electron Microscopy (SEM) experiments were performed on a JSM-7600F microscope with digital image acquisition.

RESULTS AND DISCUSSION

The XRD spectrum of CuO-SnO₂ (CS) and CuO-SnO₂-Fe₂O₃(CSF) are depicted below (Fig. 1 a and b). The XRD pattern shows extent of crystallization of the CuO-SnO₂ and CuO-SnO₂-Fe₂O₃. Different phases were observed in powder diffraction patterns of CS and CSF. A small shoulder diffraction peak was recognized as a tetragonal phase of SnO₂ at $2\theta=26^\circ$. The XRD pattern shows the presence of both CuO-SnO₂ and CuO-SnO₂-Fe₂O₃ in the sample.

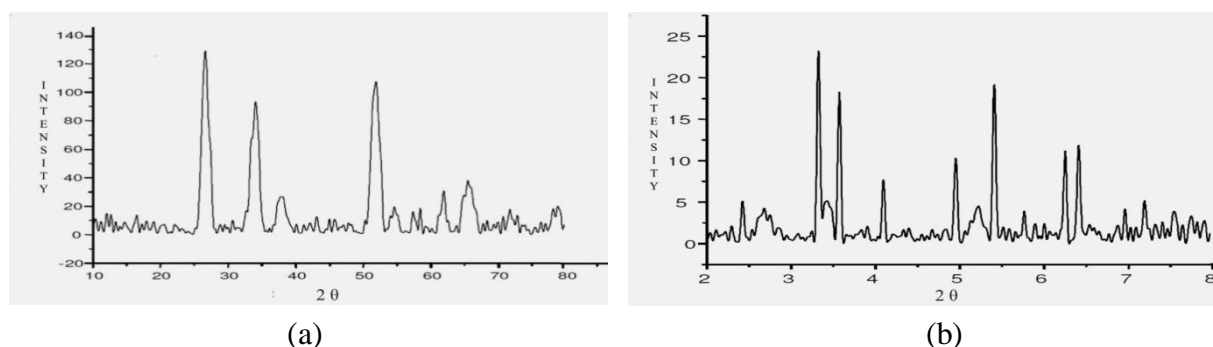


Fig. 1. XRD pattern of CuO-SnO₂ (a) and CuO-SnO₂-Fe₂O₃ powder (b)

Fourier transform Infrared spectrum (FT-IR) of CuO-SnO₂ (Fig. 2 a) shows strong absorption at 579 cm⁻¹ due to the Cu-O vibration. The intense bands were observed at 1626 and 3445 cm⁻¹, it could be due to hydrated compounds.

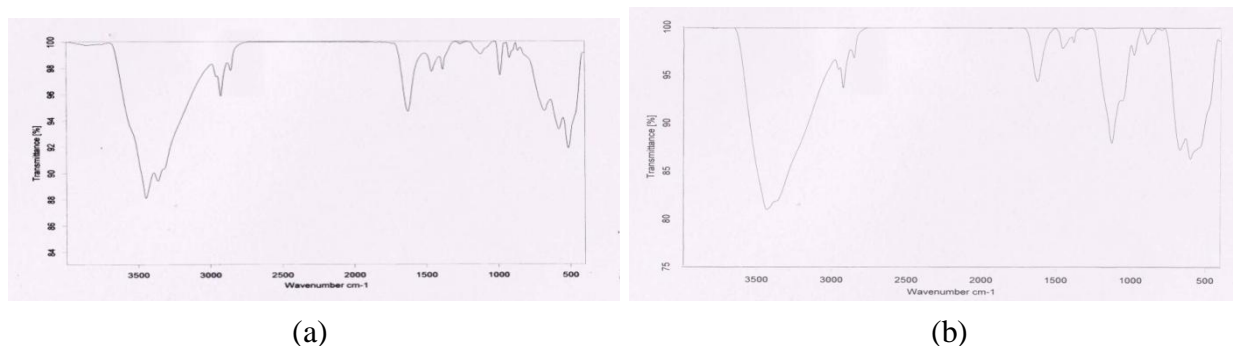


Fig. 2. FT-IR of (a) CuO-SnO₂ and (b) CuO-SnO₂-Fe₂O₃

FT-IR spectrum of CS in the $\nu(\text{OH})$ region) shows one broad band around $3300\text{--}3800\text{ cm}^{-1}$, this band corresponds to $-\text{OH}$ stretching vibrations of surface hydroxyl groups. The Peaks observed at 2924 cm^{-1} , 1460 cm^{-1} and 1360 cm^{-1} it could be due to Cu-O interaction.

Fourier transform Infrared spectrum (FT-IR) of $\text{CuO-SnO}_2\text{-Fe}_2\text{O}_3$ (**Fig. 2 b**) shows strong absorption at 601 cm^{-1} and 671 cm^{-1} due to the Cu-O and Sn-O vibrations respectively. The intense bands were observed at 1625 and 3434 cm^{-1} , it could be due to hydrated compounds.

FT-IR spectrum of CSF in the $\nu(\text{OH})$ region) shows one broad band around $2993\text{--}3450\text{ cm}^{-1}$, this band corresponds to $-\text{OH}$ stretching vibrations of surface hydroxyl groups. The Peaks observed at 2924 cm^{-1} , 1460 cm^{-1} and 1360 cm^{-1} it could be due to Cu-O interaction. The Peaks observed at 881 cm^{-1} , 891 cm^{-1} and 1127 cm^{-1} it could be due to Fe-O interaction.

The thermal stability of the prepared sample was investigated by TGA/DTA method. Thermogravimetric analysis (TGA) and Differential Thermal Analysis (DTA) were applied to the precursor hydroxide to determine the temperature for conversion of the precursors to CuO-SnO_2 and $\text{CuO-SnO}_2\text{-Fe}_2\text{O}_3$. Both measurements were carried out from 50°C to 650°C at a heating rate of 5°C min^{-1} . The analysis of CuO-SnO_2 (**Fig. 3 a**) showed that the thermal decomposition consists of two major exothermic peaks in the Differential thermal curve indicating that the hydroxides are thermally stable up to nearly 195°C . TG profile was characterized by two peaks of weight loss till 420°C . The first one occurs at 185°C . The second weight loss occurred between 420°C . DTA profile showed two decompositions.

The analysis of $\text{CuO-SnO}_2\text{-Fe}_2\text{O}_3$ (**Fig. 3 b**) showed that the thermal decomposition consists of three major exothermic peaks in the Differential thermal curve indicating that the hydroxides are thermally stable up to nearly 162°C . TG profile was characterized by three peaks of weight loss till 587°C . The first one occurs at 239°C . The second and third weight loss occurred at 395°C and 587°C respectively. DTA profile showed three decompositions.

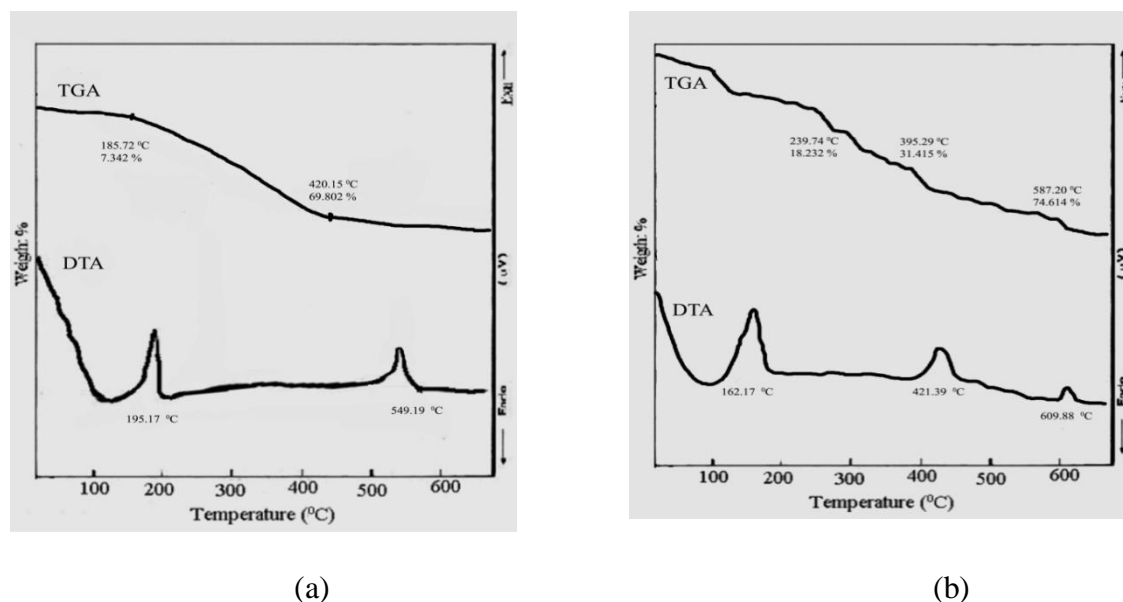


Fig. 3. TG-DTA of (a) CuO-SnO_2 and (b) $\text{CuO-SnO}_2\text{-Fe}_2\text{O}_3$

Scanning Electron Microscopy (SEM) experiments were performed on a JSM- 7600F. From SEM images it is clear that CuO-SnO_2 and $\text{CuO-SnO}_2\text{-Fe}_2\text{O}_3$ particles were obtained in nano size range and showed

uniform-sized particles with somewhat spherical morphology with an average size range of 20 – 35 nm. SEM images of CuO-SnO₂ (Fig. 4) and CuO-SnO₂-Fe₂O₃ (Fig. 5) are depicted.

APPLICATIONS

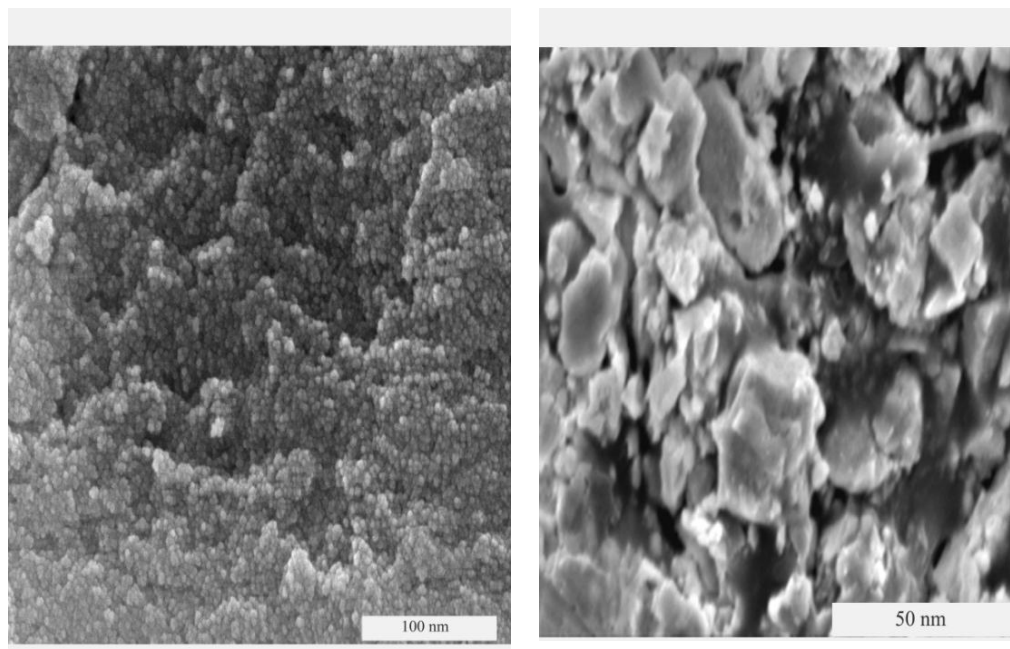


Fig. 4. SEM images of CuO-SnO₂ at 100 and 50 nm

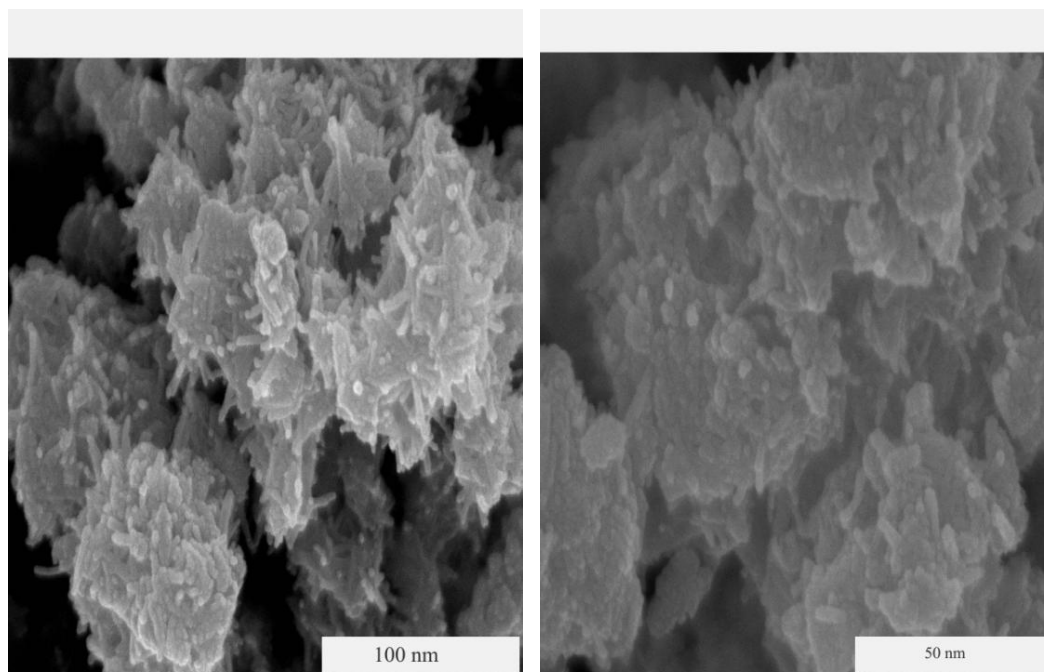


Fig. 5. SEM images of CuO-SnO₂-Fe₂O₃ at 100 and 50 nm

CONCLUSIONS

We synthesized CuO-SnO₂ and CuO-SnO₂-Fe₂O₃ mixed oxides by hydrothermal method. The obtained XRD results showed that single phase double oxide compounds were the main components in each case. SEM images showed the formation of either platelet or well defined polyhedron crystal structures based on the type of the double oxide and the preparation method.

ACKNOWLEDGEMENT

Author is thankful to SAIF, IIT Bombay for availing the spectral data.

REFERENCES

- [1] a) H. H. Kung, Transition Metal Oxides: Surface Chemistry and Catalysis; *Stud. Surf. Sci. Catal.*, Elsevier, Amsterdam, **1989**, 45, 1–277, (b) V. E. Henrich and P. A. Cox, The Surface Science of Metal Oxides, Cambridge University Press, Cambridge, UK, **1994**, (c) C. Noguera, Physics and Chemistry at Oxide Surface, Cambridge University Press, Cambridge, UK, (1996), (d) S. U. Sonavane, M. B. Gawande, S. S. Deshpande and R. V. Jayaram, *Catal. Commun.*, **2007**, 8, 1803.
- [2] G. C. Bond, Catalysis by Metals, Academic Press, New York, **1962**.
- [3] (a) C. Mercier, P. Chabardes, Heterog. Catal. Fine Chem., III, *Stud. Surf. Sci. Catal.*, **1993**, 78, 677, (b) Y. Izumi, N. Natsume, H. Takamine, I. Tamaoki and K. Urabe, *Bull. Chem. Soc. Jpn.*, **1989**, 62, 2159, (c) K. Tanabe and W. F. Holderich, *Appl. Catal., A*, **1999**, 181, 399, (d) B. M. Reddy and A. Khan, *Catal. Rev. Sci. Eng.*, **2005**, 47, 257.
- [4] S. U. Sonavane and R. V. Jayaram, *Synlett*, **2004**, 146.
- [5] M. A. Pena and J. L. G. Fierro, *Chem. Rev.*, **2001**, 101, 1981.
- [6] (a) H. Kanai, Y. Ikeda and S. Imamura, *Appl. Catal., A*, 2003, 247, 185; (b) S. K. Samantaray and K. Parida, *Appl. Catal., A*, **2001**, 220, 9.
- [7] S. D. Jackson and J. S. J. Hargreaves, Metal Oxide Catalysis, Wiley-VCH, ISBN-10: 3527318151, **2008**.
- [8] S. V. Merzlikin, N. N. Tolkachev, L. E. Briland, T. Strunskus, C. Wall, I. E. Wachs, G. Wolfgang, *Angew. Chem. Int. Ed.*, **2010**, 49, 8037.
- [9] J. Geserick, T. Froschl, N. Husing, G. Kucerova, M. Makosch, T. Diemant, S. Eckle, R. J. Behm, *Dalton Trans.*, **2011**, 40, 3269.
- [10] S. M. Saqer, D. I. Kondarides, X. E. Verykios, *Appl. Catal. B: Environ*, **2011**, 103, 275.
- [11] J. A. Rodriguez, D. Stacchiola, *Phys. Chem. Chem. Phys.*, **2010**, 12, 9557.
- [12] J. B. Park, J. Graclani, J. Evans, D. Stacchiola, S. Ma, P. Liu, A. Nambu, J. F. Sanz, J. Hrbek, J. A. Rodriguez, *PNAS*, **2009**, 116, 4975.
- [13] J. J. Yu, X. P. Wang, L. D. Li, Z. P. Hao, G. Q. Xu, (Max) Lue, *Adv. Funct. Mater*, **2007**, 17, 3598.
- [14] C. Lucarelli, P. Moggi, F. Cavani, M. Devillers, *Appl. Catal. A: Gen.*, **2007**, 325, 24.
- [15] L.J.I. Coleman, W. Epling, R. R. Hudgins, E. Croiset, *Appl. Catal. A: Gen.*, **2009**, 363, 52.
- [16] H. Cui, M. Zayat, D. J. Levy, *Sol-Gel Sci. Techn*, **2005**, 35, 175.
- [17] A. Elia, A. P. Martin, N. Quaranta, J. M. Martin, P. Vazquez, *Macromol. Symp*, **2011**, 301, 136.
- [18] Y. J. Kim, S. B. Rawal, S.D. Sung, W. I. Lee, *Bull. Korean Chem. Soc.*, **2011**, 32, 141.
- [19] B. M. Reddy, B. Chowdhury, P. G. Smirniotis, *Appl. Catal. A: Gen.*, **2001**, 211, 19.
- [20] G. C. Sankar, N. R. Rao, T. J. Rayment, *Mater. Chem.*, **1991**, 1, 299.
- [21] A. Tang, H. Yang, X. Zhang, *Int. J. of Phys. Sci.*, **2006**, 1, 101.
- [22] S. Ajaikumar, A. Pandurangan, *Applied Catalysis A: General*, **2009**, 357, 184.
- [23] W. C. Sheets, E. S. Stampler, H. Kabbour, M. I. Bertoni, L. Cario, T. O. Mason, T. J. Marks, K. R. Poeppelmeier, *Inorg. Chem.*, **2007**, 46, 10741.
- [24] D. Jiang, L. Su, L. Ma, N. Yao, X. Xu, H. Tang, X. Li, *Appl. Surf. Sci.*, **2010**, 256, 3216.
- [25] B. M. Reddy, I. J. Ganesh, *Mol. Catal. Chem. A.*, **2001**, 169, 207.

- [26] G. K. Pradhan, K. M. Parida, *Int. J. Engin. Sci. and Tech.*, **2010**, 2, 53.
- [27] M. Zhang, T. An, X. Hu, C. Wang, G. Sheng, J. Fu, *Appl. Catal. A: Gen*, **2004**, 260, 215.
- [28] M. Zhang, G. Sheng, J. Fu, T. An, X. Wang, X. Hu, *Mater. Lett.*, **2005**, 59, 3641.
- [29] H. Abimanyu, B. S. Ahn, C.S. Kim, K. S. Yoo, *Ind. Eng. Chem. Res.*, **2007**, 46, 7936.
- [30] I. E. Wachs, K. Routray *ACS Catal*, **2012**, 2, 1235–1246.
- [31] R. A. Kadir, Z. Li, A. Z. Sadek, R. A. Rani, A. S. Zoolfakar, R. M. Field, J.Z. Ou, A.F. Chrimes, K. Kalantar-zadeh *J. Phys. Chem. C*, **2014**, 118, 3129–3139.